Published online 5 July 2016

Nucleic Acids Research, 2016, Vol. 44, No. 17 ***e139***
doi: 10.1093/nar/gkw580

Next-generation RNA-based fluorescent biosensors enable anaerobic detection of cyclic di-GMP

Xin C. Wang[1], Stephen C. Wilson[2] and Ming C. Hammond[1,2,*]

[1]Department of Molecular & Cell Biology, University of California, Berkeley, CA 94720, USA and [2]Department of Chemistry, University of California, Berkeley, CA 94720, USA

Received January 22, 2016; Revised May 28, 2016; Accepted June 16, 2016

ABSTRACT

Bacteria occupy a diverse set of environmental niches with differing oxygen availability. Anaerobic environments such as mammalian digestive tracts and industrial reactors harbor an abundance of both obligate and facultative anaerobes, many of which play significant roles in human health and biomanufacturing. Studying bacterial function under partial or fully anaerobic conditions, however, is challenging given the paucity of suitable live-cell imaging tools. Here, we introduce a series of RNA-based fluorescent biosensors that respond selectively to cyclic di-GMP, an intracellular bacterial second messenger that controls cellular motility and biofilm formation. We demonstrate the utility of these biosensors *in vivo* under both aerobic and anaerobic conditions, and we show that biosensor expression does not interfere with the native motility phenotype. Together, our results attest to the effectiveness and versatility of RNA-based fluorescent biosensors, priming further development and application of these and other analogous sensors to study host–microbial and microbial–microbial interactions through small molecule signals.

INTRODUCTION

Fluorescent biosensors are invaluable tools in cell biology research, allowing researchers to detect and monitor ions, small molecules, pH, and voltage potential, all in real time (1). In particular, genetically encoded sensors, such as those derived from green fluorescent protein (GFP) or related proteins, can be expressed and detected in the native cellular environment, a crucial advantage when studying cellular response and signaling *in vivo* (2). Their fluorescence, however, depends on the formation of an amino acid-based chromophore via a maturation process that requires molecular oxygen (3,4). The need for oxygen makes them ill-suited for anaerobic applications, where they suffer from reduced or variable brightness and slow turn-on kinetics (5). Alternatively, proteins that fluoresce upon binding to endogenous chromophores, such as the flavin-binding iLOV (6,7) or the bilirubin-binding UnaG (8), hold promise for anaerobic applications. However, the scope of biosensors derived from these protein scaffolds remains very small compared to that of GFP (1,9–11).

The recently developed Spinach aptamer is a genetically encodable RNA aptamer whose fluorescence also derives from binding to an external chromophore called DFHBI that has been shown to diffuse into cultured bacterial and mammalian cells (12–14). We and others have shown that small molecule-responsive fluorescent biosensors can be engineered by fusing the Spinach aptamer to another detection aptamer, such that fluorescence turn-on occurs only in the presence of the ligand (15–18). Thus, we hypothesized that these types of biosensors could be advantageous for anaerobic applications, as they should not need oxygen to fluoresce.

Previously, our lab developed Vc2-Spinach (hereafter referred to as Vc2), a biosensor that responds to the bacterial second messenger cyclic di-GMP (c-di-GMP) (16). Predicted to be a signaling molecule in 75% of all sequenced bacteria (19), c-di-GMP regulates biofilm formation, host colonization, and bacterial virulence (20,21), affirming its profound role in microbial ecology and host–pathogen interactions. These c-di-GMP regulated processes are likely to influence the composition of microbes found in the anaerobic environment of the human digestive tract (22,23). Furthermore, c-di-GMP synthases and phosphodiesterases have been linked to oxygen-sensing domains, suggesting that oxygen directly regulates c-di-GMP levels (24–26). However, the lack of a robust tool to measure c-di-GMP levels *in vivo* has prevented any direct analysis to date.

Here, we report a series of second-generation biosensors that are up to 450% brighter and 13 times faster than Vc2, which together enable detection of c-di-GMP from picomolar to micromolar concentrations. To our knowledge, this study demonstrates the first live-cell measurement of cyclic di-GMP under anaerobic conditions. Furthermore, we show that expression of the RNA-based biosensor does not affect motility, a c-di-GMP regulated phenotype. Beyond advancing tools for the study of c-di-GMP signaling,

*To whom correspondence should be addressed. Tel: +1 510 642 0509; Email: mingch@berkeley.edu

© The Author(s) 2016. Published by Oxford University Press on behalf of Nucleic Acids Research.
This is an Open Access article distributed under the terms of the Creative Commons Attribution License (http://creativecommons.org/licenses/by-nc/4.0/), which permits non-commercial re-use, distribution, and reproduction in any medium, provided the original work is properly cited. For commercial re-use, please contact journals.permissions@oup.com

these results highlight the potential of RNA-based biosensors for both aerobic and anaerobic imaging applications.

MATERIALS AND METHODS

General reagents and oligonucleotides

Cyclic dinucleotides used in this study were purchased from Axxorra, LLC (Farmingdale, NY, USA). DFHBI and DFHBI-1T were synthesized as previously described (14,15) and stored as a ∼30 mM stock in DMSO. All GEMM-I-Spinach DNA oligonucleotides were purchased from Integrated DNA Technologies (IDT, Coralville, IA, USA), while other oligonucleotides were purchased from Elim Biopharmaceuticals (Hayward, CA, USA). All oligos are listed in Supplementary Table S1.

Bioinformatic analysis of GEMM-I variants

The GEMM-I riboswitch aptamer variants employed in the phylogenetic screen were selected as previously described (17). Briefly, sequences were extracted from Rfam database (accession RF01051, http://rfam.xfam.org/, 27) and were ranked, sorted and selected with respect to various criteria including but not limited to: folding stabilization energies, presence of specific c-di-GMP binding pocket residues, host organism and source, evolutionary position, tractability of the P1 stem, and downstream genes. The phylogenetic sequences themselves are listed in Supplementary Table S2, while the Spinach flanking sequences Supplementary Table S3.

Molecular cloning

For *in vivo* expression, biosensors were flanked by a tRNA scaffold and cloned into the BglII and XhoI sites of pET31b(+) as previously described (16,17,28) using the tSp2- and p31b- primers listed in Supplementary Table S3. YhjH was amplified from *E. coli* BL21 Star genomic DNA, and its sequence and WspR alleles (16) were cloned into the NdeI and XhoI sites of pCOLADUET-1. The two plasmids encoding the biosensor and enzyme were co-transformed into *E. coli* BL21 (DE3) Star cells (Life Technologies). For motility assay experiments, the Ct biosensor and enzymes were cloned into pETDuet-1 via Gibson assembly for dual expression from a single plasmid. The T7promoter-tRNA-Ct-terminator fragment was amplified from the pET31b vector constructs using dSens-primers (Supplementary Table S3), while T7promoter–enzyme fragments were amplified from the pCOLADuet constructs with the dWspR- and dYhjH- primers. The vector was a fragment of the pETDuet-1 vector cut at the NdeI and XhoI positions, and the three pieces were assembled with the Gibson Assembly Master Mix (New England Biolabs, Ipswich, MA, USA).

Fluorescent proteins were cloned into pET31b(+). GFP-LVA has a LVA degradation tag at the C-terminal end and was a gift from the Guillemin Lab at the University of Oregon (Eugene, OR, USA); the protein was cloned into pET31b(+) between the NdeI and XhoI restriction sites. The iLov sequence (6) was ordered as a gBlock from IDT (Coralville, IA, USA) and cloned into pET31b(+) between the NdeI and SalI restriction sites.

In vitro fluorescence assays

All biosensor and Spinach RNAs used for *in vitro* fluorescence activation assays were prepared as previously described (29). Briefly, DNA templates were first amplified with the appropriate Spinach or Spinach2 primer pairs. Transcriptions were performed using T7 RNA polymerase and the RNA product purified by a denaturing (7.5 M urea) 6% PAGE gel. RNA was eluted from the gel, precipitated, dried and resuspended in water. Accurate RNA quantitation was obtained by thermal hydrolysis (30).

Fluorescence activation assays were performed as previously described (16,17,28). Briefly, each reaction consisted of RNA, ligand and DFHBI in a binding buffer consisting of 40 mM HEPES, 125 mM KCl and 3 or 10 mM $MgCl_2$ at pH 7.5. RNA was refolded in binding buffer before being added to the binding reaction. The reaction plate was incubated at the appropriate temperature and fluorescent measurements were taken on a SpectraMax Paradigm plate reader (Molecular Devices) at 448 nm excitation/506 nm emission. Reported fluorescence values are for reactions that have reached equilibrium, as defined by fluorescence level stabilization over time. For ligand selectivity experiments, fluorescence values were normalized to biosensor with c-di-GMP. For DFHBI titration experiments, fluorescence values were background-subtracted, with background defined as fluorescence of buffer, ligand and DFHBI without RNA. All other values are reported in raw form.

In vitro fluorescence turn-on kinetics

For kinetics experiments, a reaction containing 10 μM DFHBI and 50 μM c-di-GMP in binding buffer was pre-incubated in the dark to 30 °C. RNA was refolded in binding buffer and pre-incubated separately to the same temperature. Fluorescence measurements were taken every 15 s as described above, starting immediately after the addition of RNA to the reaction mixture. There was an approximate dead time of 15 s between RNA addition and the first fluorescence reading. Fluorescence values were then normalized against maximum fluorescence exhibited for each biosensor.

Flow cytometry analysis of *in vivo* fluorescence

Flow cytometry experiments were carried out as previously described (17). Briefly, fresh LB/Carb/Kan cultures were started from overnight cultures, and cells were grown to an OD_{600} ∼0.3 and biosensor and enzyme expression was induced with 1 mM IPTG at 37 °C for 3 h. Cells were then diluted 1:30 in 1x PBS containing 50 μM DFHBI and fluorescence was measured for at least 10 000 events using a BD Fortessa X20 flow cytometer equipped with a 488 nM laser and a 530/30 filter in the Flow Cytometry Core Facility at the University of California at Berkeley. Data were analyzed with FlowJo (version 10.0.7).

Flow cytometry analysis (anaerobic growth and oxygen recovery)

Anaerobic cultures were grown in Balch tubes in ZYP-5052 autoinduction media (31) supplemented with Carb/Kan. Cultures were inoculated aerobically and the tubes were

capped with a chlorobutyl rubber stopper and crimped with an aluminum seal. The headspace was then sparged with argon for >15 min to ensure anaerobic conditions. Cells were grown while shaking for ∼15 h at 37 °C until cells reached an OD_{600} > 3. Each tube was then individually opened and the cultures immediately diluted 1:70 into 70 μl of 1x PBS pH 7.5 with 100 μM DFHBI-1T and fluorescence of 50 000 events analyzed on an Attune NxT flow cytometer (Life Technologies) equipped with a 488 nm laser for excitation and 515/15 filter for emission.

For oxygen recovery, cultures were briefly agitated after breaking the anaerobic seal, then placed at 4 °C, loosely capped, for 2 h before taking an identical fluorescence measurement in the flow cytometer. Data were analyzed with FlowJo (version 10.0.7).

Motility assays

Escherichia coli MG1655 cells were transformed with constructs by electroporation and grown overnight in liquid culture. Following published protocols (32), culture densities were adjusted to $OD_{600} = 4$ and 3 μl of culture was spotted onto agar plates containing 0.5% tryptone, 0.5% NaCl, 0.3% agar and 20 μM IPTG. Plates were allowed to air dry at room temperature for 30 min before being inverted and placed at 28 °C for 15 h. Plate images were analyzed with ImageJ (NIH, Bethesda, MD, USA).

RESULTS

Anaerobic growth affects GFP but not RNA aptamer fluorescence

To confirm that Spinach-based systems could function anaerobically, we expressed the aptamer in anaerobically cultured *E. coli* BL21 Star cells. Bacteria expressing the second-generation Spinach2 (13) exhibited 4.0-fold brighter fluorescence than bacteria expressing the oxygen-dependent GFP-LVA (Figure 1A). The LVA degron tag was added to ensure that measured fluorescence came from recently synthesized GFP (33). The fluorescence levels of cells expressing Spinach2, as well as those expressing the flavin-binding iLOV, remained consistent after cells were exposed to ambient oxygen. On the other hand, the fluorescence of GFP-expressing cells increased 13.2-fold after oxygen exposure, confirming its oxygen sensitivity and incompatibility with anaerobic applications.

Next, we considered whether the c-di-GMP biosensor Vc2 (16) could function anaerobically. Initial *in vitro* evaluation of Vc2, however, indicated that its maximum brightness was only 19.9% that of Spinach2, suggesting that the sensor would perform poorly *in vivo* under the challenging anaerobic conditions (Figure 1B). That fact, coupled with Vc2's slow fluorescence turn-on kinetics (16) (Supplementary Figure S1, Figure 3C), prompted us to develop second-generation Spinach-based biosensors for c-di-GMP.

Phylogenetic and P2 stem screens identify four second-generation biosensors

We first screened other natural riboswitches as the ligand-binding aptamer. Bioinformatics analysis of riboswitches from the c-di-GMP-binding GEMM-I class yielded a phylogenetic sequence library, from which 52 sequences were selected for screening. Corresponding riboswitch-Spinach fusions were designed, synthesized and evaluated for fluorescence response to two concentrations of c-di-GMP (Figure 2, Supplementary Figure S2). Ct256-Spinach, derived from *Clostridium thermocellum*, and Dp17-Spinach, derived from *Deinococcus proteolyticus*, were selected for high fluorescence turn-on (4.3- and 3.3-fold, respectively, with 50 μM c-di-GMP) and fast fluorescence activation. These fold activation values are impressive given the low concentrations of the biosensors (30 nM) and represent a significant improvement over Vc2-Spinach, which exhibits only 1.5-fold turn-on under identically stringent conditions (3 mM Mg^{2+} and 37 °C).

To further increase biosensor brightness, we replaced the dye-binding Spinach aptamer with the improved Spinach2 sequence that has 1.5-fold higher fluorescence than the original Spinach aptamer (13). Maximal fluorescence for Vc2-Spinach2, Ct256-Spinach2 (referred to as Ct) and Dp17-Spinach2 (referred to as Dp) were enhanced to similar extents over their Spinach counterparts (between 1.5- and 1.9-fold). Meanwhile, c-di-GMP binding affinity remained constant for Vc2 (Supplementary Figure S3). Vc2-Spinach2, Ct and Dp showed 2.9-, 6.7- and 6.0-fold fluorescence turn-on, respectively, at 30 nM biosensor and 50 μM c-di-GMP. In contrast, Spinach2 alone does not respond to c-di-GMP, nor do biosensors with mutations in a riboswitch stem that disrupt its folding (Ct-M and Dp-M) (Figure 3A).

The transducer pairing stem (P2) that lies at the interface between the Spinach and riboswitch aptamers affects ligand binding affinity and fluorescence turn-on (15). Thus, changing the transducer stem serves as another strategy to improve the biosensor. A survey of different P2 sequences of varying lengths and thermodynamic stabilities did not yield brighter biosensors than Ct and Dp (Supplementary Figure S4). However, a similar survey for the *Paenibacillus lactis*-derived Pl156-Spinach, which exhibited a 1.9-fold turn-on in the original phylogenetic screen, yielded two improved biosensors: Pl-A-Spinach2 (referred to as Pl-A), with a 7 base-pair transducer stem and 5.0-fold turn-on, and Pl-B-Spinach2 (referred to as Pl-B), with a 4 base-pair transducer stem and 4.2-fold turn-on (Figure 3A, Supplementary Figure S4). Non-binding mutants of the biosensors (Pl-A-M and Pl-B-M) again showed minimal response to c-di-GMP.

Second-generation biosensors are brighter than parent Spinach2

Through screening the phylogenetic and P2 stem libraries (a total of 68 constructs), we identified four second-generation biosensors with improved brightness and fluorescence turn-on that span a range of binding affinities for c-di-GMP (Figure 3B, Supplementary Figure S5). This suite of biosensors is responsive from 10% to 90% signal from <400 pM to 2.5 μM c-di-GMP, which is about four orders of magnitude in c-di-GMP concentrations. The biosensors also maintain selectivity toward c-di-GMP versus all other cyclic di-nucleotides and related compounds (Supplementary Figure S6). The two highest-affinity biosensors, Ct and Pl-B, respond to high concentrations of pGpG, a linear cleav-

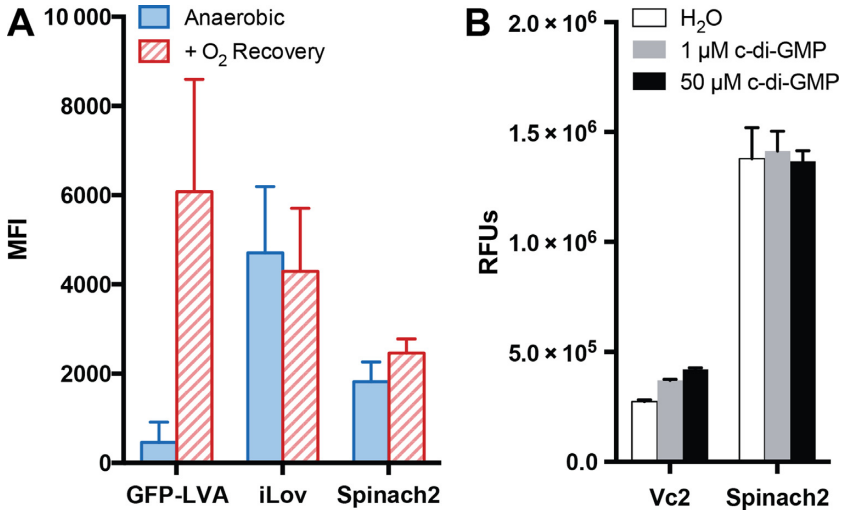

Figure 1. Fluorescence under anaerobic growth and oxygen recovery. (**A**) Average mean fluorescence intensity (MFI) measured by flow cytometry of *E. coli* BL21 (DE3) Star cells expressing GFP-LVA, iLOV or Spinach2 constructs. These cells also co-express an inactive enzyme WspR G249A to control for expression load to match later experiments (see Figure 5), where cells express both biosensor and enzyme. Solid bars denote fluorescence after anaerobic growth; patterned bars denote fluorescence after oxygen recovery. Data are from 3 independent replicates (50 000 cells/run) represented as mean ± SD. (**B**) Fluorescence activation of Vc2 and Spinach2 *in vitro* with different concentrations of c-di-GMP, as measured in relative fluorescence units (RFUs).

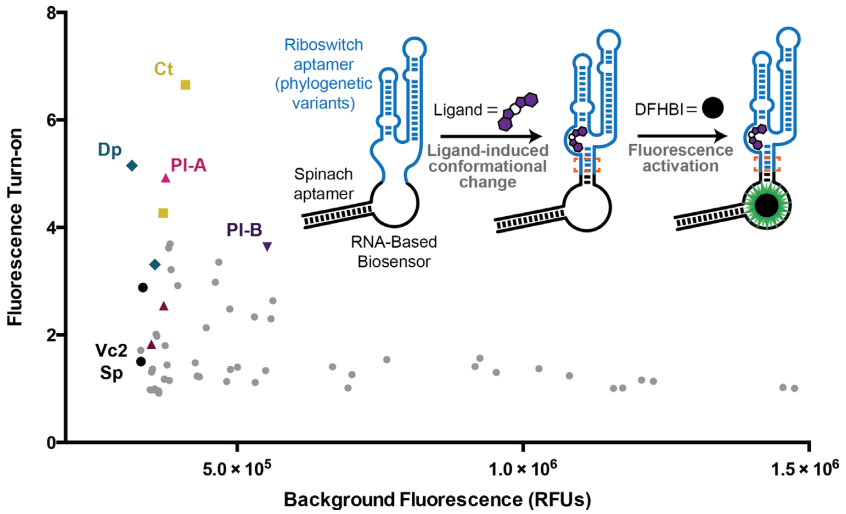

Figure 2. Screens identify four second-generation biosensors for cyclic di-GMP. Select data from the original GEMM-I-Spinach phylogenetic screen (Supplementary Figure S2) plotted with respect to background fluorescence (x-axis), defined as fluorescence with no c-di-GMP, versus fluorescence turn-on (y-axis), defined as ratio of fluorescence with 50 μM c-di-GMP over with no c-di-GMP. The original Vc2-Spinach and second-generation biosensors (Ct, Dp, Pl-A, Pl-B) are labeled as shown. Unlabeled points of corresponding shape and color indicate performance of original Spinach (not Spinach2) counterparts, as well as the original WT Pl transducer stem variant. **Inset:** General scheme for ligand-responsive RNA-based fluorescent biosensors. Full sequences are shown in Supplementary Table S2 and secondary structure models are shown in Supplementary Figure S5.

age product of c-di-GMP specific phosphodiesterases, but the biosensors still are ∼2000-fold selective for c-di-GMP, as each biosensor's fluorescence response to 100 nM c-di-GMP is similar to that with 50 μM pGpG (Supplementary Figure S6C). These biosensors are also less affected by changes in temperature and Mg^{2+} concentration than Vc2-Spinach (Supplementary Figure S7). Furthermore, these biosensors all activate in response to c-di-GMP at least 13 times more rapidly than Vc2-Spinach ($t_{1/2}$ = 1–1.5 min for new biosensors, $t_{1/2}$ = 20.25 min for Vc2-Spinach) (Figure 3C, Supplementary Figure S1).

Impressively, our second-generation biosensors have maximal fluorescence levels brighter than that of Spinach2 itself (106–143%, Figure 3A). This is in stark contrast to other published Spinach–riboswitch fusion biosensors, all of which exhibit considerably lower fluorescence (15–18,34). We found that the new biosensors, when saturated with ligand, have tighter apparent binding affinities to DFHBI than Spinach2 alone (Supplementary Figure S8), which has the effect of increasing dye occupancy. While increased brightness of Spinach2 was attributed to higher folding stability relative to Spinach (13), we did not find a consistent trend

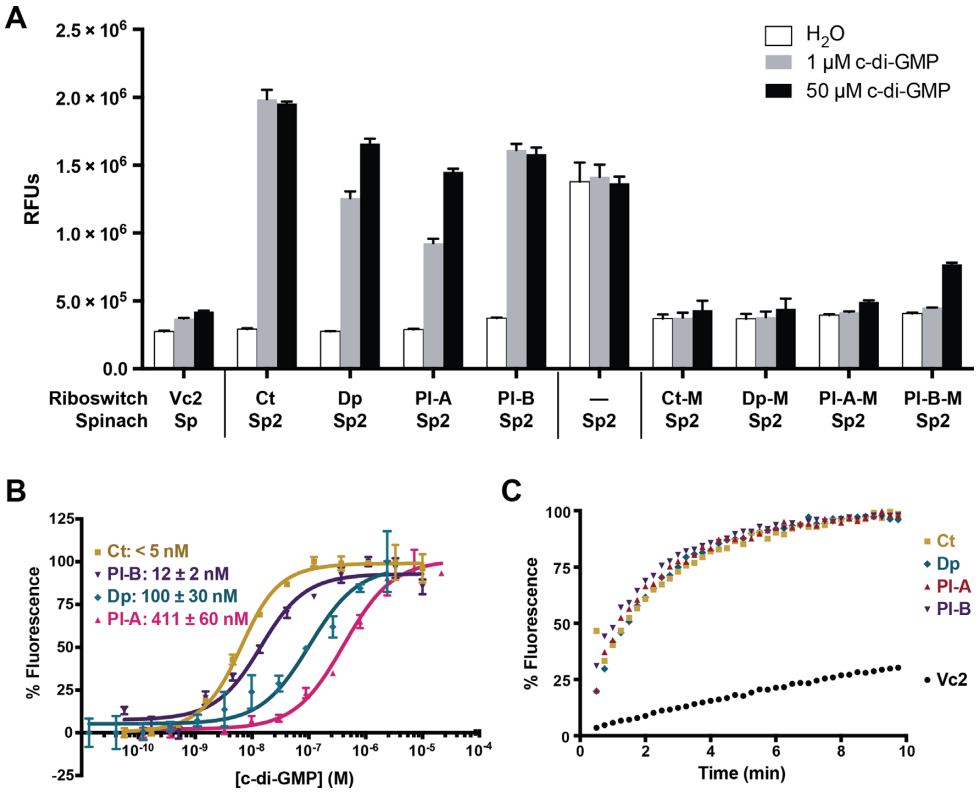

Figure 3. *In vitro* characteristics of second-generation biosensors. (**A**) Fluorescence activation of different biosensors constructs and Spinach2, with 0, 1 μM and 50 μM c-di-GMP. Data are from 3 independent replicates represented as mean ± SD. (**B**) Biosensor binding affinity measurements are shown as % maximum fluorescence, normalized for each biosensor, with titration of c-di-GMP at 3 mM Mg^{2+}, 37 °C. Calculated dissociation constant values are shown. Data are from 3 independent replicates represented as mean ± SD. (**C**) Biosensor fluorescence turn-on kinetics are shown as % maximum fluorescence, which is normalized for each biosensor. Data shown are the means from 3 independent replicates. Error bars were omitted for clarity.

in analyzing the folding stabilities of the biosensors versus Spinach2 (Supplementary Figure S9).

Taken together, the *in vitro* results suggest that these second-generation biosensors would function much better than Vc2-Spinach *in vivo*. To perform this comparison, we co-expressed the new biosensors in aerobically grown *E. coli* with enzymes that affect cellular c-di-GMP concentrations, and analyzed live cell fluorescence by flow cytometry (Figure 4). In general, the histograms showed relatively uniform distribution of fluorescence and, by proxy, c-di-GMP levels in the bacterial cell population. However, more heterogeneity in the distribution could be seen with extended expression times (Supplementary Figure S10). While Vc2-expressing cells showed no significant fluorescence turn-on upon co-expression of the constitutively active cyclic di-GMP synthase WspR D70E, all cells expressing second-generation biosensors exhibited fluorescence turn-on, indicating robust responses to high c-di-GMP concentrations. Furthermore, consistent with the *in vitro* measurements, maximal fluorescence levels for the new biosensors were higher than that for Spinach2 (111–175%) analyzed under identical conditions, including WspR co-expression to equalize the expression load. The two most sensitive biosensors, Ct and Pl-B, also displayed significant fluorescence activation in response to endogenous c-di-GMP levels, as indicated by higher fluorescence levels upon co-expression of an inactive enzyme, WspR G249A, versus YhjH, a c-di-GMP-specific phosphodiesterase ($P = 0.043$ and 0.053, respectively).

RNA-based fluorescent biosensors function under anaerobic conditions

We tested the ability of Ct, the brightest and highest affinity biosensor, to detect c-di-GMP under anaerobic conditions (Figure 5). The biosensor maintained responsiveness to c-di-GMP, as fluorescence turn-on was observed with WspR D70E co-expression. Intriguingly, fluorescence levels were the same for cells co-expressing the inactive WspR G249A or YhjH phosphodiesterase, which is in contrast to observations made under aerobic growth conditions. This result likely reflects lower endogenous c-di-GMP levels under anaerobic conditions, as oxygen activates the *E. coli* c-di-GMP synthase DosC (24) and anaerobic promoters upregulate expression of the *E. coli* c-di-GMP-specific phosphodiesterase YfgF (25). Also consistent with these expected effects, a 1.54-fold increase in fluorescence was observed for cells co-expressing WspR D70E after the anaerobic culture was exposed to ambient oxygen for 2 h at 4 °C.

The fluorescence signal for the control, Spinach2, does increase by 1.35-fold after oxygen recovery as well. Therefore, the fluorescence increase upon oxygen recovery may also be partially attributed to differences in biosensor expression or steady-state levels under these conditions. Nevertheless, it

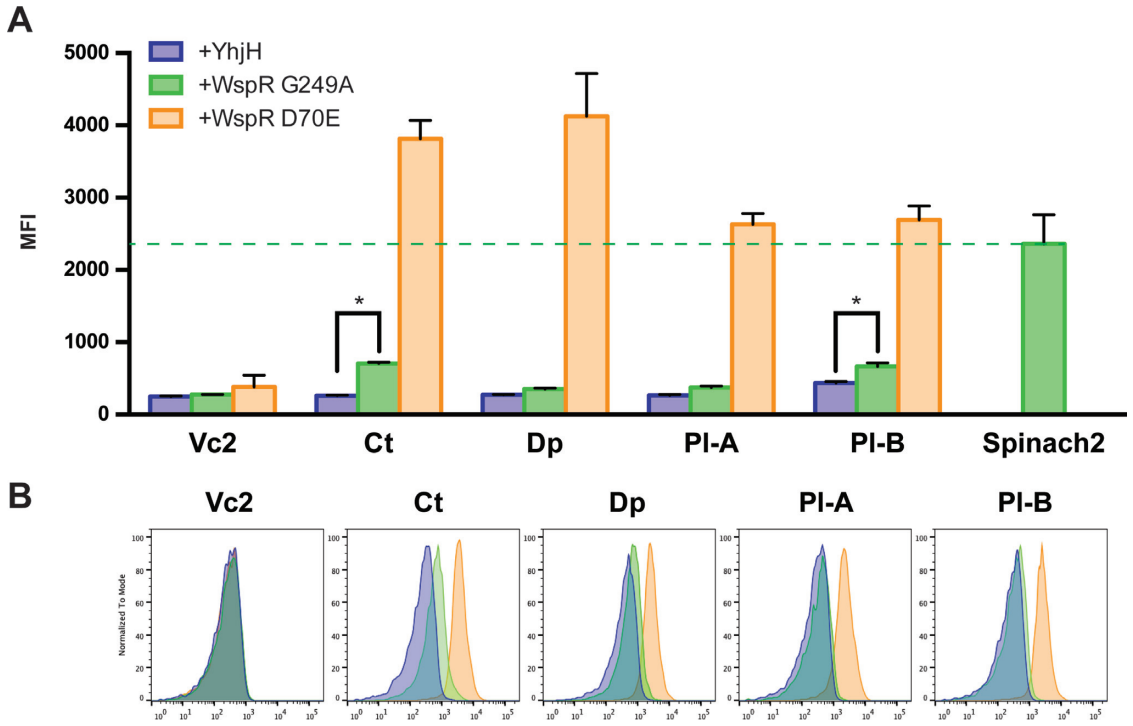

Figure 4. Second-generation biosensors are brighter than Spinach2 *in vivo*. (**A**) Average mean fluorescence intensity (MFI) measured by flow cytometry of *E. coli* BL21 (DE3) Star cells co-expressing indicated biosensor constructs or Spinach2, along with various enzymes. Blue denotes phosphodiesterase YhjH; green denotes inactive mutant of diguanylate cyclase WspR (G249A); orange denotes constitutively active mutant of WspR (D70E). Data are from 3 independent replicates (10 000 cells/run) represented as mean ± SD. (**B**) Representative flow cytometry graphs for samples shown in part **A**.

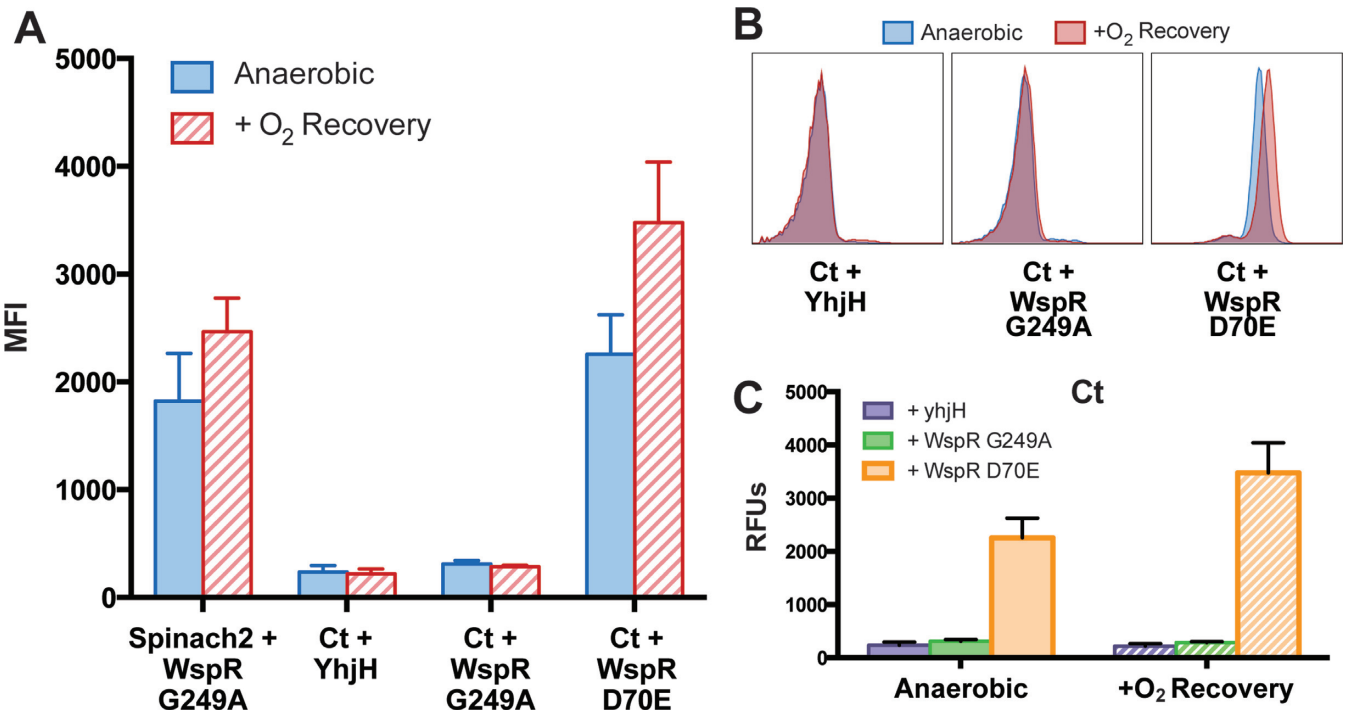

Figure 5. Cyclic di-GMP biosensors function under anaerobic conditions. (**A**) Average MFI measured by flow cytometry of *E. coli* BL21 (DE3) Star cells co-expressing Spinach2 or Ct, along with various c-di-GMP perturbing enzymes. Solid bars denote fluorescence after anaerobic growth; patterned bars denote fluorescence after oxygen recovery. Data are from 3 independent replicates (50 000 cells/run) represented as mean ± SD. Data are from 3 independent replicates (50 000 cells/run) represented as mean ± SD. (**B**) Representative flow cytometry graphs for samples shown in part **A**. (**C**) Same data as in part **A** rearranged to compare fluorescence with co-expression of different c-di-GMP perturbing enzymes.

is clear that compared to the fluorescent protein GFP-LVA (13.2-fold), RNA-based fluorescent biosensors are less dependent on oxygen for fluorescence, and thus have great potential utility for measuring endogenous signals or metabolites *in vivo* under anaerobic conditions.

Expression of RNA-based biosensor does not affect motility phenotype

Two general criticisms leveled at biosensors for live-cell applications are the saturation effect, in which excess target saturates biosensor signal, and the observer effect, in which biosensor binding sequesters the cellular pool of target ligands, thereby altering the phenotype (35). We intended to circumvent the saturation effect by making a suite of four sensors with different binding affinities, thus ensuring a wide dynamic range of almost four orders of magnitude. To assay for potential observer effect, we examined the impact of biosensor expression on cellular motility, a phenotype regulated by cellular c-di-GMP levels in *E. coli*. High levels of c-di-GMP lead cells to transition from motile to sessile states. Accordingly, cells expressing the active synthase WspR D70E exhibit little to no motility in soft agar, while cells expressing the phosphodiesterase YhjH are more motile than cells with presumed wild-type levels of c-di-GMP, which either carry the empty pCOLA vector or express the inactive WspR G249A to account for protein expression (Figure 6A).

Cells expressing Spinach2, our highest affinity biosensor Ct or the non-binding mutant Ct-M all exhibit similar motilities as the empty vector and WspR G249A controls. However, it appears that wild-type levels of c-di-GMP are quite low under these growth conditions that may make the observer effect difficult to assess. Thus, in a separate experiment, we compared the motility of cells co-expressing Ct with WspR WT versus cells expressing WspR WT alone. Cells expressing WspR WT have an intermediate level of c-di-GMP as determined using our first- and second-generation biosensors (16) (Supplementary Figure S11). Accordingly, cells expressing WspR WT have an intermediate motility phenotype that is not significantly affected by co-expression of the highest affinity biosensor Ct (Figure 6B). This lack of observer effect could be due to faster turnover of RNA-based biosensors that alleviates ligand sequestration. In contrast, cells expressing the c-di-GMP binding protein YcgR exhibit reduced motility, as this c-di-GMP effector acts to bind flagellar proteins and stop flagellar motion (36).

DISCUSSION

This latest series of RNA-based fluorescent biosensors significantly improve upon the original Vc2 biosensor toward detecting c-di-GMP in live cells. They provide much higher fluorescence signal and faster activation, and also offer a range of binding affinities, with the highest affinity biosensor capable of detecting sub-nanomolar concentrations of c-di-GMP. We screened for biosensors with increased fold turn-on by analyzing the fluorescence signal at 30 nM RNA, a concentration lower than the 100 nM used in earlier experiments (16). The second-generation biosensors can now be used in flow cytometry experiments to detect endogenous c-di-GMP levels, as well as low, medium and high levels due to co-expression of YhjH phosphodiesterase and different alleles of WspR synthase, respectively. We recently applied the Dp biosensor in a successful high-throughput screen for c-di-GMP synthase activity (37). Going forward, the relatively high fluorescence signal of these biosensors means that lower expression levels are needed for *in vivo* imaging of c-di-GMP signaling, which is advantageous for future applications in different strains of *E. coli* and other bacteria. So far, we have found that DFHBI and related DFHBI-1T dyes are readily permeable in cultured *E. coli* and *Listeria monocytogenes* cells (18) as model Gram negative and positive bacteria, respectively. However, it may be necessary to test dye permeability for other bacterial species. The activation kinetics of these biosensors are on the minute timescale ($t_{1/2} = 1$–1.5 min) that should be acceptable for monitoring dynamic changes in c-di-GMP levels associated with physiologically relevant processes, such as cell division in *Caulobacter crescentus* (38). Notably, this current screen did not deliberately optimize for turn-on kinetics, and we expect there is still room for improvement.

The Ct and Pl-B biosensors have extremely tight binding affinities for c-di-GMP, maintaining $\geq$2000-fold selectivity against similar ligands. These biosensors respond to micromolar concentrations of the linear dinucleotide pGpG *in vitro*, but they did not show significant fluorescence signal in *E. coli* expressing the phosphodiesterase YhjH (Figure 4) that produces pGpG from endogenous c-di-GMP. This result suggests that pGpG levels in *E. coli* MG1655 are quite low. Some bacterial strains have been reported to have high levels of pGpG; for instance, the PA14 strain of *Pseudomonas aeruginosa* contains 11 μM of pGpG and 20-fold lower concentration of c-di-GMP, while mutants deficient for oligoribonuclease, which hydrolyzes pGpG into two GMP molecules, have even higher concentrations of pGpG (39). Since we have shown that ligand specificity can be reprogrammed with structure-based mutagenesis of RNA-based biosensors (16,28), it may be possible to develop a biosensor selective for pGpG, which could prove useful for measuring the activity of pGpG-metabolizing enzymes.

Finally, we demonstrate the ability of these biosensors to function *in vivo* under anaerobic conditions. While more work is needed to correlate fluorescence levels with exact c-di-GMP concentrations, these new biosensors open the door to studying c-di-GMP signaling in live bacteria, irrespective of the environmental oxygen content. This is particularly relevant to functional studies of gut microbiota that occupy partial to fully anaerobic niches. For future imaging experiments in animal gut models, it would be important to test methods of administering the dye and potentially make other DFHBI analogs that will enable the study of c-di-GMP signaling *in situ*.

In addition, we demonstrate that Spinach2 itself can function under anaerobic conditions, extending the known utility of this aptamer that has been validated for live imaging of RNA and protein expression *in vivo* (13,40). We propose that Spinach2 or related aptamer-dye pairs can be used to observe changes in gene expression under differential oxygen conditions, a known phenomenon yet to be mon-

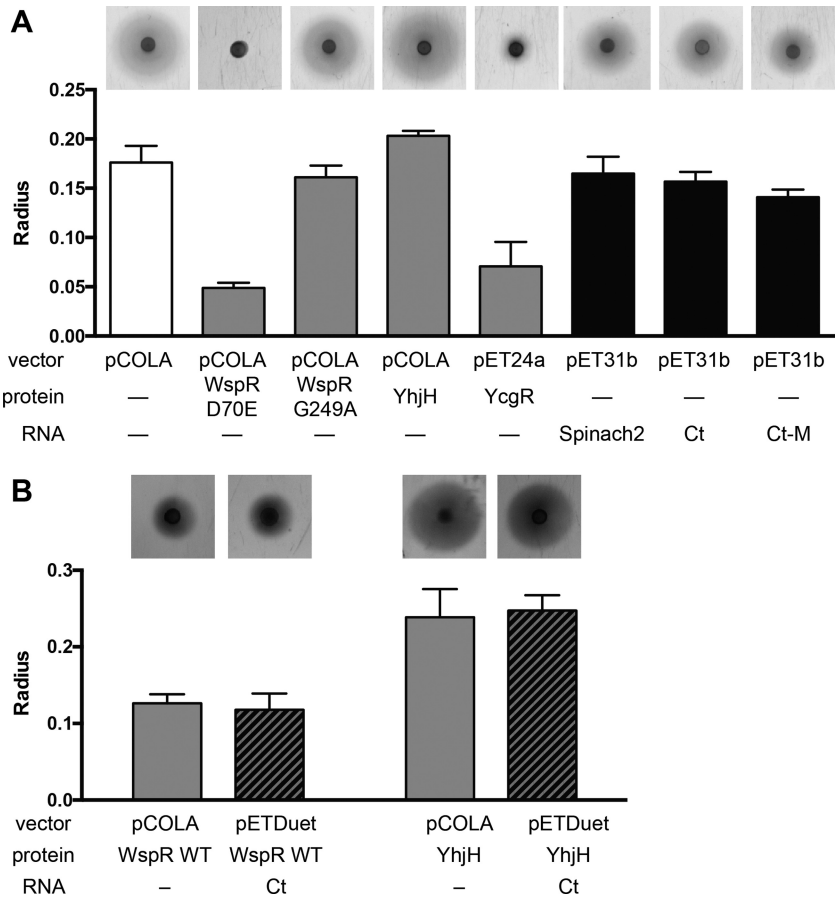

Figure 6. Biosensor expression does not disrupt motility phenotype. (**A**) Representative photos of motility zones for *E. coli* MG1655 cells in soft agar are shown above the analysis graph of the calculated radii for cells expressing empty plasmid (white), enzymes (grey) or RNAs (black). Data are from 3 independent replicates represented as mean ± SD. (**B**) Same as in part **A** for cells expressing enzyme alone (solid) or enzyme and Ct biosensor (striped). Data are from 2 independent replicates represented as a mean ± SD.

itored in real time (41). Taken together, our results highlight the potential of aptamer-dye pair based methods for tracking RNAs, metabolites or soluble signals under variable oxygen conditions that can provide new insights into how cells adapt to changes in environmental oxygen availability.

This current study further reinforces several design principles for creating riboswitch-based Spinach biosensors. Namely, our results demonstrate that sampling the phylogenetic diversity of natural riboswitches provides an efficient strategy for surveying functional sequence space, similar to natural enzyme variants forming the starting point for directed evolution in protein engineering (42). The aptamer portions of the four second-generation biosensors share only 37–66% nucleotide sequence identity and include several insertions and deletions, a level of diversity not easily achieved via random mutagenesis (Supplementary Figure S12). This type of sequence diversity would be present in a random sequence library, but the phylogenetic approach is considerably more efficient, as the 68 sequences we assayed to efficiently arrive at four biosensors that all function *in vivo* is considerably less than the total number of unique sequences in a corresponding random library.

We recently described first-generation RNA-based fluorescent biosensors for live cell imaging of other signaling molecules, including c-di-AMP (18) and c-AMP-GMP (17). Our experience with designing, synthesizing and now optimizing these types of biosensors have established the following general principles: (i) accurate knowledge of aptamer secondary structure is important for rational design of the transducer stem (18); (ii) stringent screening conditions, including accurate measurement of RNA concentrations (30), are critical to comparing and optimizing biosensor performance; and (iii) sampling diverse sequences enables different solutions to the folding problem, yielding better biosensors (this study). The strong performance characteristics displayed by these second-generation c-di-GMP biosensors under both aerobic and anaerobic conditions, along with the potential to engineer riboswitch- or aptamer-based biosensors for other small molecules or proteins, should inspire others to join in the use and development of this promising biosensor technology.

SUPPLEMENTARY DATA

Supplementary Data are available at NAR Online.

ACKNOWLEDGEMENTS

The authors thank C. Kellenberger for laying the groundwork for many of the experiments performed, J. Gallagher and C. Chen for advice on anaerobic experiments, Z. Hallberg for motility assay advice and Z. Hallberg and Y. Su for helpful discussions.

FUNDING

National Institutes of Health (NIH) [DP2 OD008677 to M.C.H]. Funding for open access charge: NIH [DP2 OD008677 to M.C.H].

Conflict of interest statement. None declared.

REFERENCES

1. Crone,D.E., Huang,Y.M., Pitman,D.J., Schenkelberg,C., Fraser,K., Macari,S. and Bystroff,C. (2013) GFP-based biosensors. In: Rinken,T (ed). *State of the Art in Biosensors - General Aspects*. InTech, Rijeka.
2. Enterina,J.R., Wu,L. and Campbell,R.E. (2015) Emerging fluorescent protein technologies. *Curr. Opin. Chem. Biol.*, **27**, 10–17.
3. Reid,B.G. and Flynn,G.C. (1997) Chromophore formation in green fluorescent protein. *Biochemistry*, **36**, 6786–6791.
4. Craggs,T.D. (2009) Green fluorescent protein: structure, folding and chromophore maturation. *Chem. Soc. Rev.*, **38**, 2865–2875.
5. Ransom,E.M., Ellermeier,C.D. and Weiss,D.S. (2015) Use of mCherry red fluorescent protein for studies of protein localization and gene expression in Clostridium difficile. *Appl. Environ. Microbiol.*, **81**, 1652–1660.
6. Drepper,T., Eggert,T., Circolone,F., Heck,A., Krauss,U., Guterl,J.-K., Wendorff,M., Losi,A., Gärtner,W. and Jaeger,K.-E. (2007) Reporter proteins for in vivo fluorescence without oxygen. *Nat. Biotechnol.*, **25**, 443–445.
7. Chapman,S., Faulkner,C., Kaiserli,E., Garcia-Mata,C., Savenkov,E.I., Roberts,A.G., Oparka,K.J. and Christie,J.M. (2008) The photoreversible fluorescent protein iLOV outperforms GFP as a reporter of plant virus infection. *Proc. Natl. Acad. Sci. U.S.A.*, **105**, 20038–20043.
8. Kumagai,A., Ando,R., Miyatake,H., Greimel,P., Kobayashi,T., Hirabayashi,Y., Shimogori,T. and Miyawaki,A. (2013) A bilirubin-inducible fluorescent protein from eel muscle. *Cell*, **153**, 1602–1611.
9. Buckley,A.M., Petersen,J., Roe,A.J., Douce,G.R. and Christie,J.M. (2015) LOV-based reporters for fluorescence imaging. *Curr. Opin. Chem. Biol.*, **27**, 39–45.
10. Erapaneedi,R., Belousov,V.V., Schäfers,M. and Kiefer,F. (2016) A novel family of fluorescent hypoxia sensors reveal strong heterogeneity in tumor hypoxia at the cellular level. *EMBO J.*, **35**, 102–113.
11. Liem,P.H., Mu,A., Kikuta,S.-I., Ohta,K., Kitajima,S. and Taketani,S. (2015) A simple and highly sensitive method of measuring heme oxygenase activity. *Biol. Chem.*, **396**, 1265–1268.
12. Paige,J.S., Wu,K.Y. and Jaffrey,S.R. (2011) RNA mimics of green fluorescent protein. *Science*, **333**, 642–646.
13. Strack,R.L., Disney,M.D. and Jaffrey,S.R. (2013) A superfolding Spinach2 reveals the dynamic nature of trinucleotide repeat–containing RNA. *Nat. Methods*, **10**, 1219–1224.
14. Song,W., Strack,R.L., Svensen,N. and Jaffrey,S.R. (2014) Plug-and-play fluorophores extend the spectral properties of Spinach. *J. Am. Chem. Soc.*, **136**, 1198–1201.
15. Paige,J.S., Nguyen-Duc,T., Song,W. and Jaffrey,S.R. (2012) Fluorescence imaging of cellular metabolites with RNA. *Science*, **335**, 1194–1194.
16. Kellenberger,C.A., Wilson,S.C., Sales-Lee,J. and Hammond,M.C. (2013) RNA-based fluorescent biosensors for live cell imaging of second messengers cyclic di-GMP and cyclic AMP-GMP. *J. Am. Chem. Soc.*, **135**, 4906–4909.
17. Kellenberger,C.A., Wilson,S.C., Hickey,S.F., Gonzalez,T.L., Su,Y., Hallberg,Z.F., Brewer,T.F., Iavarone,A.T., Carlson,H.K., Hsieh,Y.-F. *et al.* (2015) GEMM-I riboswitches from Geobacter sense the bacterial second messenger cyclic AMP-GMP. *Proc. Natl. Acad. Sci. U.S.A.*, **112**, 5383–5388.
18. Kellenberger,C.A., Chen,C., Whiteley,A.T., Portnoy,D.A. and Hammond,M.C. (2015) RNA-based fluorescent biosensors for live cell imaging of second messenger cyclic di-AMP. *J. Am. Chem. Soc.*, **137**, 6432–6435.
19. Seshasayee,A.S.N., Fraser,G.M. and Luscombe,N.M. (2010) Comparative genomics of cyclic-di-GMP signalling in bacteria: post-translational regulation and catalytic activity. *Nucleic Acids Res.*, **38**, 5970–5981.
20. Ryan,R.P. (2013) Cyclic di-GMP signalling and the regulation of bacterial virulence. *Microbiology*, **159**, 1286–1297.
21. Römling,U., Galperin,M.Y. and Gomelsky,M. (2013) Cyclic di-GMP: the first 25 years of a universal bacterial second messenger. *Microbiol. Mol. Biol. Rev.*, **77**, 1–52.
22. Lozupone,C.A., Stombaugh,J.I., Gordon,J.I., Jansson,J.K. and Knight,R. (2012) Diversity, stability and resilience of the human gut microbiota. *Nature*, **489**, 220–230.
23. Nicholson,J.K., Holmes,E., Kinross,J., Burcelin,R., Gibson,G., Jia,W. and Pettersson,S. (2012) Host-gut microbiota metabolic interactions. *Science*, **336**, 1262–1267.
24. Tuckerman,J.R., Gonzalez,G., Sousa,E.H.S., Wan,X., Saito,J.A., Alam,M. and Gilles-Gonzalez,M.-A. (2009) An oxygen-sensing diguanylate cyclase and phosphodiesterase couple for c-di-GMP control. *Biochemistry*, **48**, 9764–9774.
25. Lacey,M.M., Partridge,J.D. and Green,J. (2010) Escherichia coli K-12 YfgF is an anaerobic cyclic di-GMP phosphodiesterase with roles in cell surface remodelling and the oxidative stress response. *Microbiology*, **156**, 2873–2886.
26. An,S., Wu,J. and Zhang,L.-H. (2010) Modulation of Pseudomonas aeruginosa biofilm dispersal by a cyclic-Di-GMP phosphodiesterase with a putative hypoxia-sensing domain. *Appl. Environ. Microbiol.*, **76**, 8160–8173.
27. Griffiths-Jones,S., Bateman,A., Marshall,M., Khanna,A. and Eddy,S.R. (2003) Rfam: an RNA family database. *Nucleic Acids Res.*, **31**, 439–441.
28. Ren,A., Wang,X.C., Kellenberger,C.A., Rajashankar,K.R., Jones,R.A., Hammond,M.C. and Patel,D.J. (2015) Structural basis for molecular discrimination by a 3′, 3′-cGAMP sensing riboswitch. *Cell Rep.*, **11**, 1–12.
29. Kellenberger,C.A. and Hammond,M.C. (2015) In vitro analysis of riboswitch-Spinach aptamer fusions as metabolite-sensing fluorescent biosensors. *Meth. Enzymol.*, **550**, 147–172.
30. Wilson,S.C., Cohen,D.T., Wang,X.C. and Hammond,M.C. (2014) A neutral pH thermal hydrolysis method for quantification of structured RNAs. *RNA*, **20**, 1153–1160.
31. Studier,F.W. (2005) Protein production by auto-induction in high density shaking cultures. *Protein Expr. Purif.*, **41**, 207–234.
32. Wolfe,A.J. and Berg,H.C. (1989) Migration of bacteria in semisolid agar. *Proc. Natl. Acad. Sci. U.S.A.*, **86**, 6973–6977.
33. Andersen,J.B., Sternberg,C., Poulsen,L.K., Bjorn,S.P., Givskov,M. and Molin,S. (1998) New unstable variants of green fluorescent protein for studies of transient gene expression in bacteria. *Appl. Environ. Microbiol.*, **64**, 2240–2246.
34. Strack,R.L. and Jaffrey,S.R. (2013) New approaches for sensing metabolites and proteins in live cells using RNA. *Curr. Opin. Chem. Biol.*, **17**, 651–655.
35. Haugh,J.M. (2012) Live-cell fluorescence microscopy with molecular biosensors: what are we really measuring? *Biophys. J.*, **102**, 2003–2011.
36. Paul,K., Nieto,V., Carlquist,W.C., Blair,D.F. and Harshey,R.M. (2010) The c-di-GMP binding protein YcgR controls flagellar motor direction and speed to affect chemotaxis by a 'backstop brake' mechanism. *Mol. Cell*, **38**, 128–139.
37. Hallberg,Z.F., Wang,X.C., Wright,T.A., Nan,B., Ad,O., Yeo,J. and Hammond,M.C. (2016) Hybrid promiscuous (Hypr) GGDEF enzymes produce cyclic AMP-GMP (3′, 3′-cGAMP). *Proc. Natl. Acad. Sci. U.S.A.*, **113**, 1790–1795.
38. Christen,M., Kulasekara,H.D., Christen,B., Kulasekara,B.R., Hoffman,L.R. and Miller,S.I. (2010) Asymmetrical Distribution of the Second Messenger c-di-GMP upon Bacterial Cell Division. *Science*, **328**, 1295–1297.
39. Orr,M.W., Donaldson,G.P., Severin,G.B., Wang,J., Sintim,H.O., Waters,C.M. and Lee,V.T. (2015) Oligoribonuclease is the primary

degradative enzyme for pGpG in Pseudomonas aeruginosa that is required for cyclic-di-GMP turnover. *Proc. Natl. Acad. Sci. U.S.A.*, **112**, E5048–E5057.
40. Song,W., Strack,R.L. and Jaffrey,S.R. (2013) Imaging bacterial protein expression using genetically encoded RNA sensors. *Nat. Methods*, **10**, 873–875.
41. Bueno,E., Mesa,S., Bedmar,E.J., Richardson,D.J. and Delgado,M.J. (2012) Bacterial adaptation of respiration from oxic to microoxic and anoxic conditions: Redox control. *Antioxid. Redox Signal.*, **16**, 819–852.
42. Lutz,S. (2010) Beyond directed evolution—semi-rational protein engineering and design. *Curr. Opin. Biotechnol.*, **21**, 734–737.